ACS APPLIED MATERIALS & INTERFACES

Research Article

www.acsami.org

Superhydrophobic and Oleophilic Open-Cell Foams from Fibrillar Blends of Polypropylene and Polytetrafluoroethylene

Ali Rizvi, Raymond K. M. Chu, Jung H. Lee, and Chul B. Park*

Microcellular Plastics Manufacturing Laboratory, Department of Mechanical and Industrial Engineering, University of Toronto, 5 King's College Road, Toronto, Ontario M5S 3G8, Canada

Supporting Information

ABSTRACT: Effective removal of oils from water is of global significance for environmental protection. In this study, we investigate the hydrophobicity and oleophilicity of open-cell polymer foams prepared in a continuous and scalable extrusion process. The material used to prepare the open-cell foams is a fibrillar blend of polypropylene (PP) and polytetrafluoroethylene (PTFE). Scanning electron microscopy (SEM) images of the morphology of the PP/PTFE fibrillar blend reveal that the PTFE has a fibrillar morphology in the PP matrix. SEM micrograph of the extruded foam shows the formation of an interconnected open-cell structure. Using nitrogen pycnometry, the open-cell content is estimated to be 97.7%. A typical bulk density of the open-cell foam is measured to be about 0.07 g cm^{-3} corresponding to a void fraction of 92%. Thus, a large three-dimensional space is made available for oil storage. A drop of water on the cross-section of the extruded open-cell foam forms a contact angle of 160° suggesting that the open-cell foam exhibits superhydrophobicity. The open-cell foam can selectively absorb various petroleum products, such as octane, gasoline, diesel, kerosene, light crude oil, and heavy crude oil from water and the uptake capacities range from about 5 to 24 g g^{-1}. The uptake kinetics can be enhanced by exposing the open-cell foam to high intensity ultrasound which increases the surface porosity of the thin, impervious, foam "skin" layer. The reusability of the foam can be improved by using a matrix polymer which demonstrates superior elastic properties and prevents the foams from undergoing a large permanent deformation upon compression to "squeeze out" the oil. For example, when the PP homopolymer matrix is replaced with a PP random copolymer, the permanent deformation for 10 compressive cycles is reduced from about 30% to 10%. To the best of our knowledge, these PP-based open-cell foams outperform PP-based absorbents conventionally used for oil-spill cleanup applications such as nonwoven PP fibers or melt-blown PP pads.

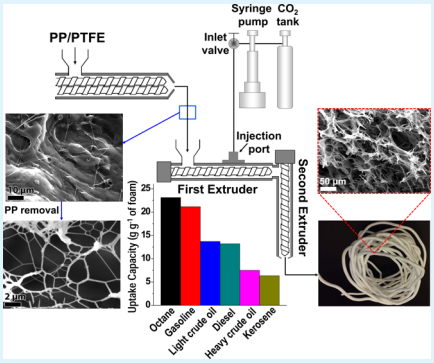

KEYWORDS: *foam, porous, open-cell, oil, extrusion*

1. INTRODUCTION

Crude oil fulfills a substantial portion of the world's energy needs. Oil exploration, extraction, transportation, storage, and usage create a risk of spillage which can be damaging to the environment. The world spends $10 billion annually on oil spill remediation.[1] There is an urgent need to develop new methods for oil spill cleanup to mitigate the adverse environmental implications, particularly because the effectiveness of the treatment depends on several factors such as oil type and weather conditions.[2] One of the most efficient and economical methods for oil spill cleanup is oil sequestering by *sorption*. The properties of an ideal absorbent for oil spill remediation include high oleophilicity and hydrophobicity to maximize the oil/water selectivity, high oil uptake capacity, high buoyancy, and low cost. Natural absorbents for oil spill cleanup include cotton,[3] milkweed,[3] wool,[4] and vegetable fibers.[5] Unfortunately, these absorbents exhibit poor oil/water selectivity due to their affinity for water limiting their effectiveness in the cleanup of oil spills. Polyurethane foams are synthetic absorbents, which have characteristics like high uptake capacities, easily scalable fabrication, and low density but also show an affinity for water.[6−8] Furthermore, they pose a waste disposal challenge as polyurethane foams are nonrecyclable and thermoset materials. Recently, porous hydrophobic and oleophilic materials (PHOMs) such as carbon-based sponges,[9,10] porous boron nitride,[11] metal−organic frameworks (MOFs),[12] and polymethylsilsesquioxane aerogels[13] have emerged as attractive alternatives in treating releases because of their excellent oil uptake capacity and selectivity. However, present studies ignore the high material cost and complex synthesis procedures to fabricate these PHOMs. The deficiencies of these existing technologies call for an urgent need to develop methods to fabricate absorbents with inexpensive, recyclable materials in a high throughput process.

Herein, we study the hydrophobic and oleophilic properties of open-cell foams prepared from fibrillar blends of polypropylene (PP) and polytetrafluoroethylene (PTFE) on a large-scale in a *continuous extrusion process*[14] capable of

Received: September 3, 2014
Accepted: November 10, 2014
Published: December 1, 2014

producing the open-cell foam at a rate of 2 kg/h (see Supporting Information, SI, Video, V1: Extrusion of open-cell PP/PTFE foams). The resulting open-cell foams comprise a three-dimensional network of interconnected solid struts that delineate cavities (known as cells), throughout the sample volume. A facile method to fabricate such foams is described and their hydrophobic properties are characterized. The uptake capacities of these foams are studied for several petroleum products such as octane, gasoline, diesel, kerosene, light crude oil, and heavy crude oil. *Ultrasound irradiation*[15−17] treatment is used to increase the porosity of the thin, impervious "skin" layer of the extruded open-cell foams, and the change in the kinetics of oil uptake by the foams before and after treatment is characterized. The reusability of the open-cell foams after oil absorption is investigated by subjecting the foams to a cyclic-compression stress−strain test as a controlled analogue for mechanical "squeezing" required for extracting the oil from the open-cell foam.

2. EXPERIMENTAL SECTION

2.1. Materials. A commercially available linear isotactic polypropylene homopolymer (PP-homopolymer) supplied by Japan Polypropylene, Novatec-PP FY4, with melt flow rate (MFR) = 5 g/10 min (at 230 °C/2.16 kg load) and poly(propylene-*co*-ethylene) random copolymer (PP-copolymer) commercially available as Sabic PP 670 K with a melt flow index (MFI) of 10 g/10 min (at 230 °C/2.16 kg load) are used as the matrix polymers in this study. The melting temperature of the PP-homopolymer is found using DSC to be about 165 °C and the PP-copolymer is found to be around 149 °C. A commercially available polytetrafluoroethylene (PTFE) powder which shows good dispersion in PP[18] and high CO_2[19] solubility supplied by Mitsubishi Rayon Company, Metablen A-3000, is also used. Carbon dioxide and nitrogen are purchased from Linde Gas with purities in excess of 99%. Diesel (Shell Ultra Low Sulfur Diesel) and gasoline (Shell Bronze Octane Number 87) are purchased from a Shell Canada Ltd. gas station. Light Crude Oil and Heavy Crude Oil are purchased from ONTA Inc. Kerosene is purchased from Canadian Tire Corporation Ltd. Octane is purchased from Caledon Laboratories Ltd. Detailed characteristics of the petroleum products are presented in Table 1. Sudan III red dye is purchased from EMD Millipore Corp.

2.2. Blend Preparation. Dry blends of the matrix polymer (either PP-homopolymer or PP-copolymer) and PTFE are prepared in proportion of 97/3 in weight fraction (wt %). The resulting mixture is fed in the hopper of a corotational twin-screw extruder manufactured by Toshiba Machine Co. Ltd. (trade name: TEM-26SS). The screw diameter is 26 mm and its aspect ratio (length/diameter) is 40. In the extruder, the fed mixture is melt-blended under a barrel and a die temperature of 200 °C but the hopper zone is cooled with a cold-water sleeve. The discharge rate is set at 20 kg/h. Extrudate from the die is shaped into a cylindrical filament, led into a cool water bath, and pelletized.

Table 1. Viscosity, Surface Tension, And American Petroleum Institute (API) Gravity of the Various Petroleum Products Used in the Study

petroleum product	viscosity (Pa·s)[a]	surface tension (N/m)[b]	API gravity (deg)[c]
octane	$<1 \times 10^{-3}$	0.022	69.4
gasoline	$<1 \times 10^{-3}$	0.025	60.3
light crude oil	0.11	0.029	36.7
diesel	2.4×10^{-3}	0.028	34.6
heavy crude oil	0.66	0.034	14.7
kerosene	2.6×10^{-3}	0.028	40.3

[a]Viscosities are measured using a Brookfield dial reading viscometer (Model LVT). Viscosities of octane and gasoline are below the detectable viscosity range using the device (minimum detectable viscosity = 1×10^{-3} Pa·s). [b]Surface tension measurements are conducted using the standard method described in ASTM D1331 at room temperature in air. [c]API gravity is determined using the formula API = (141.5/RD) − 131.5, where RD is the relative density of the petroleum product at 15.6 °C.

2.3. Foam Extrusion Procedure. A tandem foam extrusion system similar to those employed by the foam manufacturing industry is used to foam the samples. The tandem foam system comprises of two single-screw extruder barrels. The first extruder is a 5 horsepower (hp) Brabender 05−25−00 consisting of a mixing screw with a diameter of 19 mm and an aspect ratio of 30. The second extruder is a 15 hp Killion KN-150 consisting of a mixing screw with a diameter of 38.1 mm and an aspect ratio of 30. Figure 1 gives a schematic of the configuration of the extrusion system. A metered amount of CO_2 gas is injected into the melt through an injection port positioned at the first extruder.[20]

First, pallets of the blend (either PP-homopolymer/PTFE or PP-copolymer/PTFE) are fed into the first extruder barrel through the hopper. This barrel is maintained at 200 °C, a temperature above the melting temperature of the matrix polymer but below that of PTFE. The matrix polymer in the samples melts completely in the first extruder due to the temperature as well as the screw motion which causes shear heating. Then, 10 wt % CO_2 is injected into the first extruder barrel at a constant flow rate using a syringe pump. The high shear and high pressure caused by the rotating screw inside the first extruder barrel facilitates the dissolution of CO_2 in the melt through convective diffusion. This homogeneous solution enters the second extrusion barrel which is maintained at temperatures below the melting temperature of the matrix polymer. Consequently, it is in this second extrusion barrel where crystallization is initiated in the samples. Foaming of the polymer melt occurs at the die exit where the polymer/CO_2 solution is subjected to rapid depressurization resulting in the gas to undergo phase separation.[14] A brass capillary die composed of a circular pinhole with a diameter of 1.2 mm and a channel length of 10 mm is employed. The temperature of the second extruder barrel and the die is brought down and the foamed samples collected at each set temperature only after the system temperature has equilibrated.

2.4. Morphology Characterization. To observe the morphology development of PTFE after blending with the matrix polymer, the blend is dissolved in xylene and the residual PTFE examined using a scanning electron microscope (SEM, JEOL 6060). To characterize the dispersion of the PTFE fibrils in the matrix, the surface of cryogenically fractured sample of the blend is subjected to a solvent vapor etching process using xylene. Samples are exposed to xylene vapors for 2 h at 65 °C. This type of treatment preferentially etches the matrix polymer which is soluble in xylene, leading to bringing up the PTFE domains and increasing differentiation in observation. To characterize the nano-features of the PTFE domains, transmission electron microscopy (TEM JEOL 2010) is used. The adsorption-desorption isotherms, surface area, and pore size distribution of PTFE are characterized using a Quantachrome Autosorb instrument with nitrogen as the adsorbate. The average pore size distribution is determined using the BJH methods.

To observe the morphology of the foamed samples, the samples are dipped in liquid nitrogen and fractured to expose the foam structure. The fractured surface is sputter coated with platinum before observation under SEM. Final images are recorded from randomly selected areas at the magnifications indicated in the SEM micrographs. For each foamed sample, the foam density is determined using the water displacement method according to ASTM D792. Additionally, the number of bubbles per unit volume, called the cell density, is also estimated from the SEM images of the foams using the method described elsewhere.[21]

2.5. Oil Absorption Test. The oil uptake capacity, defined as the mass in grams of the oil absorbed per gram of the foam at equilibrium, is measured for various petroleum products including octane, gasoline, diesel, light crude oil, heavy crude oil, and kerosene. In a typical test, a

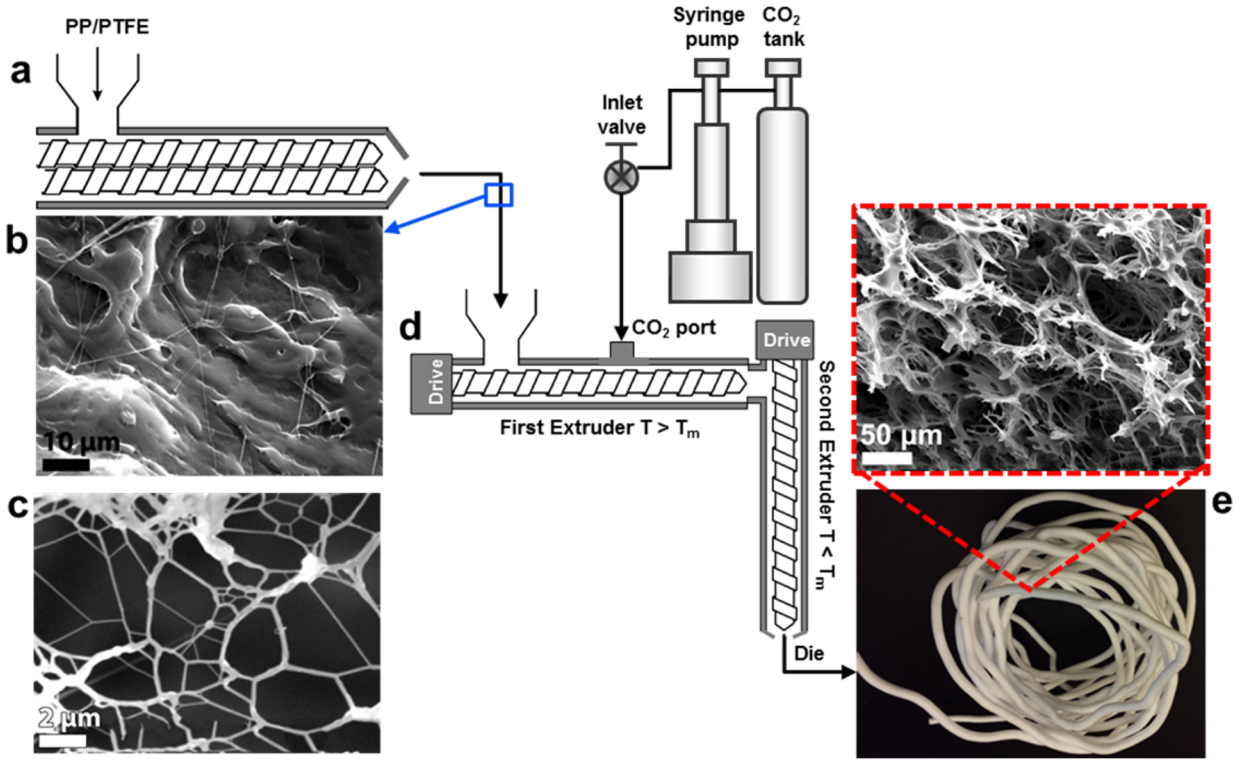

Figure 1. Schematic showing the preparation of open-cell foams from PP-homopolymer/PTFE fibrillar blends: (a) PP-homopolymer is blended with PTFE in the ratio 97 and 3 wt %, respectively, in a twin-screw extruder; (b) SEM micrograph of the twin-screw extruded blend after solvent-vapor etching using xylene. The PTFE exists as well-dispersed, high-aspect-ratio fibrils in the blend; (c) PTFE fibrils after selective removal of PP from the fibrillar blend using xylene. The PTFE fibrils form an entangled mesh-like structure; (d) the fibrillar blend is foamed in a tandem single-screw foam extrusion system.[14] The temperature of the first extruder is maintained above the T_m of PP but below that of PTFE. Ten wt % CO_2 is injected in the first extruder using a syringe pump; and (e) photograph of a continuous open-cell foam filament produced by the foam extrusion system. The open-cell foam filament is produced with a diameter of about 4 mm and can be produced at a rate of 2 kg/h. The continuous nature of the process allows the foam filament to be of a very large length exceeding hundreds of meters. The SEM micrograph (dashed outline) shows the morphology of the extruded foam filament.

dry open-cell foam sample of known mass is immersed completely into the respective petroleum product for 24 h using an external force. Subsequently, the foam is taken out and rapidly weighed to minimize the effect of evaporation of the absorbate. The uptake capacity of the foam is calculated as (mass after saturation in oil − initial mass of foam)/(initial mass of foam). The petroleum product is then extracted from the foam with the aid of a vacuum pump. This process is repeated ten times and the average uptake capacity along with the standard deviation is calculated.

To measure the kinetics of oil absorption, dry foam samples of known masses are immersed completely using an external force into the petroleum product for different time periods after which the foam samples are removed, weighed, and their uptake capacities at their respective times calculated.

2.6. Mechanical Properties of the Foam. To test the reusability of the foams, the foams are subjected to a cyclic compression test as a controlled analogue for mechanical squeezing for oil recovery. Stress–strain measurements are performed for 10 cycles on an Instron 5848 microtester equipped with a 50 N load cell. The maximum strain is set to 60% and the compression rate is set at 0.25 mm/min.

2.7. Contact Angle Determination. The contact angles of droplets (10–30 μL) of deionized water or gasoline on the cross-section of the cylindrical open-cell foams are obtained using a custom-built contact angle measurement system under room temperature and pressure. The details of the system used can be found elsewhere.[22] After capturing the boundary profile of the droplet, ImageJ software is used to determine the contact angles.

2.8. Ultrasound Treatment. The extruded foam filament is cut into cylinders of about 3 mm length and subjected to high intensity ultrasound irradiation using a commercial ultrasonic source (Sonics VCX750) with a probe diameter of 13 mm, operating at a frequency of 20 kHz and a maximum power of 750 W. The ultrasonic probe is positioned about 1 mm above the foam held in place using a rubber fixture in a bath filled with distilled water. Ultrasound pulses with an on/off ratio of 3:3 are applied to the foam with an ultrasound power intensity of 750 W for 10 min.

3. RESULTS AND DISCUSSION

3.1. Preparation of Open-Cell Foams of PP/PTFE Fibrillar Blends. We prepare open-cell foams of PP and PTFE fibrillar blends. The procedure for fabricating the open-cell foams of PP-homopolymer/PTFE is illustrated schematically in Figure 1. First, PP-homopolymer/PTFE (97/3 wt %) is blended in a twin-screw extruder at 200 °C (Figure 1a). The SEM image in Figure 1b reveals that the PTFE deforms into high aspect ratio fibrils during blending (diameter <500 nm and length >100 μm, so the aspect ratio is >200), as previously reported.[18,19,23,24] The image is obtained after solvent-vapor etching using xylene. Figure 1c shows the SEM micrograph of PTFE fibrils after the selective removal of PP from the PP/PTFE blend with xylene. The PTFE fibrils form an entangled mesh-like structure. Figure 1d shows a schematic of the tandem foam extrusion system used to foam the PP/PTFE fibrillar blend. A photograph of the extrusion system can be found in SI Figure S1. The system is able to extrude a foam filament of 4 mm diameter at a rate of 2 kg/h. In the first extruder, the blend is subjected to a temperature of 200 °C to melt the PP and 10

wt % CO_2 is injected and dissolved in the melt. In the second extruder, the PP/PTFE/CO_2 system is subjected to temperatures below the melting temperature of PP, so that the PP is able to develop *crystalline heterogeneities* in this extruder. Specifically, the occurrence of flow-induced *shish-kebab*[25] type structures during extrusion of semicrystalline polymers is reported.[1] We also observe such crystalline morphologies in the extruded PP/PTFE (see SI Figure S2). Upon foaming, cell opening is initiated when a *heterogeneous-melt structure*[26−28] characterized by well dispersed arrays of rigid and soft segments exist in the sample. The mechanisms for cell-opening initiated through the formation of a heterogeneous-melt structure has been extensively investigated and can be found elsewhere.[2] The crystalline heterogeneities of PP that develop in the second extruder are rigid relative to the molten matrix and form the structural heterogeneities needed to achieve high open-cell contents. Furthermore, the dissolution of 10 wt % CO_2 in PP/PTFE sample plasticizes the molten sections, thereby increasing the chances of opening the soft segments of the bubble walls.[27,29] There exists a processing temperature window within which the crystalline heterogeneities will yield foams with the highest open-cell content.[30] The optimum temperature for preparing foams of PP-homopolymer/PTFE with the highest open-cell content (i.e., open cell content of about 97.7%) is identified to be 150 °C. While the bulk density of the unfoamed fibrillar blend ($\rho_{unfoamed}$) is measured to be about 0.92 g cm^{-3}, the bulk density after foam extrusion (ρ_{foam}) at 150 °C drops to about 0.07 g cm^{-3}. Figure 1e shows a photograph of the extruded open-cell foam filament and the blow-up image shows the SEM of the foam cross-section which exhibits a highly porous, interconnected, 3D framework with struts that delineate cavities (or cells). The number of cells per unit volume, or cell density, is estimated from the SEM images to be between 10^7 to 10^8 cells cm^{-3}. The cell diameters are in the range of 50 to 500 μm. The void fraction, ($V_f = 1 - \rho_{foam}/\rho_{unfoamed}$), is calculated to be about 0.92. It is expected that the large void fraction of the highly porous, largely expanded, interconnected structure makes available a large 3D space for oil storage.

3.2. Morphology of the PTFE Fibrils. The TEM image in Figure 2a shows a PTFE fibril after selective removal of PP from the PP/PTFE fibrillar blend using xylene. The section of the PTFE fibril under observation has a consistent diameter and an internal structure characterized by longitudinal nanofeatures. Consequently, the BET surface area and the pore size distribution is studied. Figure 2b shows the nitrogen adsorption−desorption isotherms of the PTFE fibrils. The adsorption−desorption isotherm can be categorized as a type IV hysteresis loop observed between P/P_0 range of 0.4 to 1.0, indicating the presence of mesopores.[31] The shape of the hysteresis loop corresponds to the H3 loop type which is known to be associated with slit-like pores in the sample.[31] The adsorption is relatively high at P/P_0 approaching 1.0. Thus, both macro and mesopores are present in the sample. The corresponding pore-size distribution of the PTFE fibrils is shown in the inset and reveals that the PTFE fibrils possess mesopores with a broad size distribution ranging from 5 to 30 nm.

3.3. Superhydrophobicity of the Open-Cell Foams. Superhydrophobic materials are difficult to wet with water and are arbitrarily defined to exhibit a contact angle, θ, >150°.[32] In order to study the hydrophobicity of the extruded open-cell foam, the foam filament is cryogenically fractured into cylinders

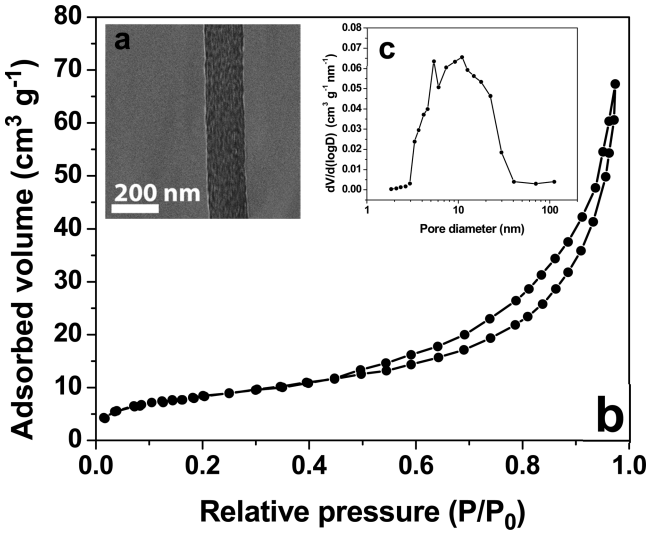

Figure 2. Morphology of the PTFE fibrils: (a) TEM image of a PTFE fibril; (b) N_2 adsorption−desorption isotherms of the PTFE fibrils; and (c) pore size distribution curve of the PTFE fibrils.

for the contact angle measurements, as shown in Figure 3a. The apparent contact angle of the cross-sectional surface of the foam with water is shown in Figure 3b and is determined to be 160° ± 0.9°. In order to compare the oleophilicity (i.e., the affinity for oil) and superhydrophobicity of the open-cell foam, a photograph is shown in Figure 3c where a water droplet forms a large contact angle on the foam, and a drop of gasoline (~12 μL) labeled with red dye is absorbed rapidly by the same foam sample. The time for absorbing a drop (~12 μL) of gasoline is only 0.73 ± 0.08 s (Figure 3d). Such rapid absorption kinetics of the open-cell foam is attributed to its highly porous structure, oleophilicity, capillary action, and the low viscosity of the gasoline. The open-cell foam continues to float on the water surface due to its low density and superhydrophobicity after oil uptake, thereby making it easy to collect the foam and extract the oil. One striking observation is the change in appearance of the open-cell foam upon immersion in water using an external force. Figure 3e shows that when the white open-cell foam is immersed in water and viewed at a glancing angle, it appears to have a silver mirror-like surface. This occurs because of the Cassie−Baxter[33] nonwetting behavior which creates a continuous air gap at the interface between the hydrophobic open-cell foam surface and water. The effect is strongest in the cross-sectional area, possibly because of a stronger hydrophobic surface than the foam skin, since a higher degree of roughness exhibits more hydrophobicity.[34] It is evident that the open-cell foam structure naturally generates sufficient roughness to impart superhydrophobicity.

The thermal stability of the open-cell foam is studied and presented in Figure 3f,g. The foam is subjected to extreme temperature environments including freezing in liquid nitrogen at −196 °C for 1 h and heating to 120 °C for 1 h. No change in the foam morphology is observed after these treatments and the open-cell foam continues to retain its superhydrophobic and oleophilic nature. When the foam is subjected to a temperature of 125 °C for 1 h, the foam morphology is not retained as the material begins to soften and distort, sacrificing the superhydrophobic characteristic of the foam. Nonetheless, the foam has a broad service temperature range of −196 to 120

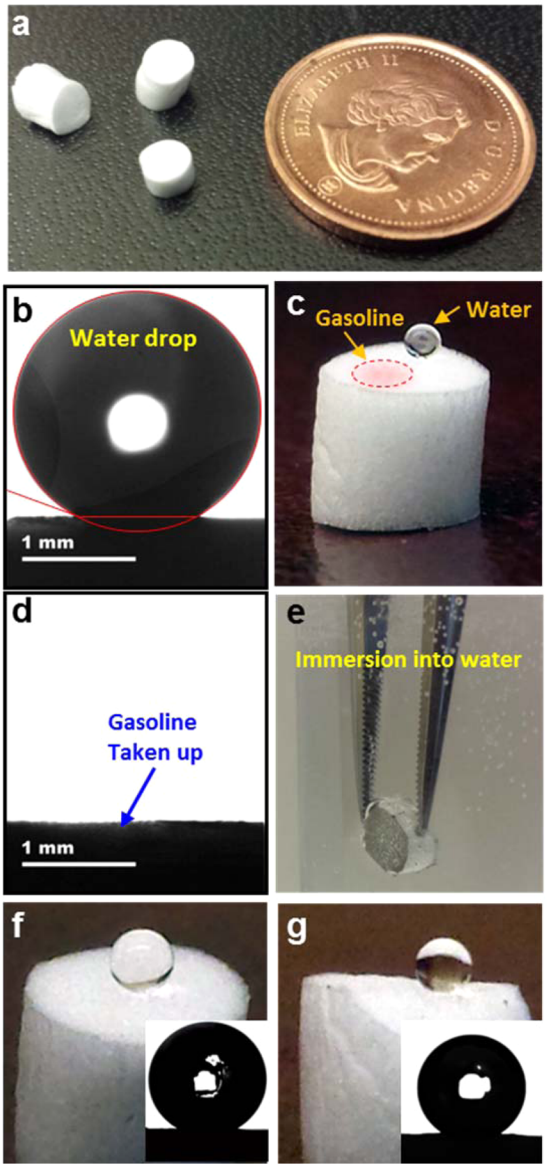

Figure 3. Superhydrophobic properties of the PP-homopolymer/PTFE open-cell foams: (a) Open-cell foam filament is cut into cylindrical shapes for testing physical properties of the open-cell foam. The diameter of the foam samples is about 4 mm and the length ranges from about 2 to 5 mm; (b) measurement of contact angle of a water droplet placed on the cross-section of the foam. The water droplet forms a contact angle of 160° ± 0.9° with foam; (c) photograph of a water drop on the cross-sectional surface of the superhydrophobic open-cell foam. A drop of gasoline labeled with a red dye is readily absorbed into the open-cell foam; (d) drop of gasoline taken up by the oil in 0.73 ± 0.08 s as observed from a video recording; (e) photograph of the open-cell foam immersed in water displaying a silver mirror-like surface when looked at from a glancing angle; and photograph of water droplet and corresponding water contact angle after subjecting the sample to (f) −196 °C and (g) 120 °C for 1 h. Superhydrophobicity of the open-cell foam is preserved after these treatments.

°C, a feature which may make the foam attractive for industrial applications beyond oil-spill cleanup and recovery.

3.4. Oil Uptake Study. PP-based oil absorbents such as nonwoven PP fibers or melt-blown PP pads are widely used for oil spill cleaning. However, these absorbents exhibit low oil uptake capacities.[35−40] Our PP-based open-cell foams are an ideal substitute for the sorption of oils and other liquid-phase organic pollutants. When a cylindrical open-cell foam sample, such as the one shown in Figure 3a, is placed on the surface of a gasoline−water mixture, the gasoline layer is readily and selectively taken up by the foam. Figure 4a shows the time lapse images of the video of oil uptake (see SI Video, V2: Oil uptake by extruded open-cell foam). To differentiate the gasoline from water, the gasoline is labeled with a red dye.

The uptake capacity of the open-cell foam is expressed in terms of the mass in grams of oil absorbed/mass in gram of foam (g g^{-1}). We study the uptake capacity of the open-cell foams for the petroleum products. First, the open-cell foam is saturated with one of these petroleum products and the gain in mass is determined to calculate the uptake capacity. Subsequently, the petroleum product is extracted with the aid of a vacuum pump. The petroleum product is recovered, and the open-cell foam regenerated for a subsequent cycle. This process is repeated ten times for all studied petroleum products. The results are shown in Figure 4b and the corresponding data are presented in Table 2. The data presented in Table 2 are also compared with literature values of uptake capacities obtained for two PP-based materials commonly used for oil spill cleanup, namely, nonwoven PP fibers and melt-blown PP pads. The physical characteristics and specifications of these PP-based materials can be found elsewhere.[38,39,41] With the exception of heavy crude oil, and kerosene, the open-cell foam outperforms these PP-based absorbents for the uptake of all other studied petroleum products. In general, the uptake capacity of the open-cell foam varies from oil to oil and ranges from around 5 to 24 g g^{-1} of foam. Furthermore, over the ten absorption/vacuum extraction cycles, the open-cell foam demonstrates consistent performance. Within experimental error, the differences in the measured uptake capacity does not change substantially as reflected from a maximum standard deviation of 1.35 g g^{-1} of foam. This result indicates that a simple vacuum extraction after saturation of the foam with the petroleum product is sufficient to recover active open-cell foam for a subsequent absorption cycle.

3.5. Effect of Mechanical Squeezing for Oil Recovery. The previous section demonstrates that vacuum extraction is effective in removing the absorbed petroleum product from the open-cell foam, to regenerate the open-cell foam for a subsequent absorption cycle. However, vacuum extraction is not ideal for oil recovery, in particular, for low viscosity petroleum products which are volatile organic liquids. For them, a *sorption-heating-condensation*[42] or a mechanical "squeezing" process needs to be employed to maximize petroleum product recovery. From a practical standpoint, the mechanical squeezing of the foam for oil extraction is a more cost-effective and scalable methodology for oil recovery. Thus, we investigate the mechanical properties of the PP open-cell foams by cyclic compression measurements as a controlled analogue of mechanical "squeezing" needed for oil recovery. Figure 5a shows cyclic compression stress−strain curves of the PP-homopolymer/PTFE open-cell foam for ten compressive cycles. The inset in Figure 5a shows the morphology of the open-cell foam. A typical stress curve increases with an increase in the applied strain. The foam is able to be compressed to a strain of 60% at a relatively low stress of 70 kPa, owing to the low density of the open-cell foam. Upon removal of the compressive force, the foam shows poor recovery to its original shape. After the first compressive cycle, the foam undergoes a

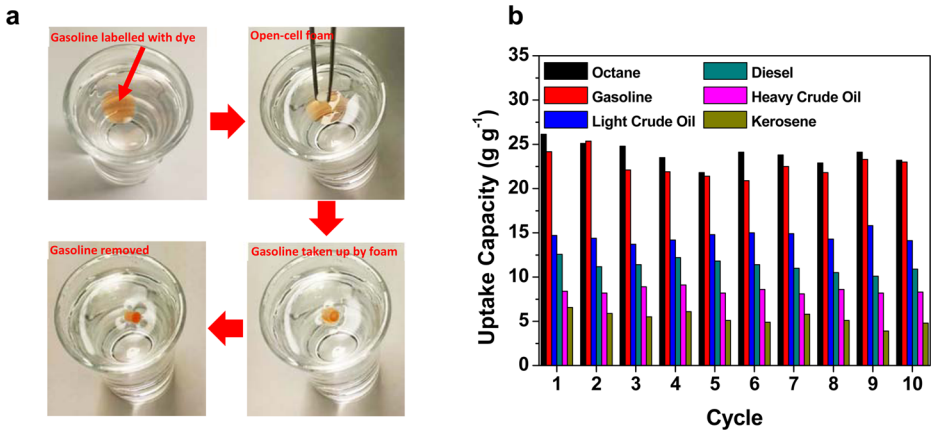

Figure 4. Uptake of various petroleum products by the open-cell polymer foams: (a) a few drops of gasoline labeled with a red dye for clear differentiation with water. The open-cell foam readily, and selectively absorbs the gasoline; (b) uptake capacity of open-cell polymer foam for various petroleum products in terms of mass in grams of oil per mass in grams of the open-cell foam (g g^{-1}). The oil is removed from the open-cell foam using vacuum pump and reused over ten cycles to study the reusability of the foams.

Table 2. Measured Uptake Capacities of the Open-Cell Foam for Various Petroleum Products and Organic Liquids[a,b]

cycle	octane	gasoline	light crude oil	diesel	heavy crude oil	kerosene
1	26.1	24.2	14.7	12.6	8.4	6.6
2	25.1	25.4	14.4	11.2	8.2	5.9
3	24.8	22.11	13.7	11.4	8.9	5.5
4	23.5	21.91	14.2	12.2	9.1	6.1
5	21.8	21.4	14.8	11.8	8.2	5.1
6	24.1	20.9	15.0	11.4	8.6	4.9
7	23.8	22.5	14.9	11.0	8.1	5.8
8	22.9	21.8	14.3	10.5	8.6	5.1
9	24.1	23.3	15.8	10.1	8.2	3.9
10	23.2	23.0	14.1	10.9	8.3	4.8
average[c]	23.9	22.6	14.6	11.3	8.5	5.4
σ[d]	1.22	1.35	0.59	0.75	0.33	0.76
literature[e]		9.2[39,f]	8.3[38,g]	9.1[39,f]	9.1[38,g]	10[41,g]

[a]The absorption time was kept constant at 24 h. [b]the uptake capacity of the foam is reported as g g^{-1} of foam. [c]Average of uptake capacities are calculated for the ten cycles. [d]σ = standard deviation. [e]Uptake capacities of various commercially available PP-based products from literature for comparison purposes. [f]Uptake capacity of commercial melt-blown PP pad. [g]Uptake capacity of commercial nonwoven PP fibers.

permanent strain of about 20%. This poor compressive fatigue behavior is attributed to the brittle nature of the PP-homopolymer matrix used in the PP- homopolymer/PTFE fibrillar blend. The brittle characteristics are a consequence of the high degree of crystallinity in linear isotactic PP-homopolymers, which occurs due to the stereoregularity of the polymer chains.[43] The impact properties of PP-homopolymers can be improved by copolymerization with ethylene. The random insertion of ethylene molecules in the PP backbone disrupts the regular, repeating structure and reduces the crystallinity compared to isotactic PP-homopolymers.[44] The lower degree of crystallinity in the copolymers imparts physical properties such as reduced stiffness, higher impact resistance and better elastic properties than PP-homopolymers.

The inadequate compressive fatigue of the PP-homopolymer/PTFE open-cell foam limits its reusability for oil uptake applications because mechanical squeezing for oil recovery will damage the morphology of the foam. When the matrix polymer used to prepare the open-cell foams is replaced from the brittle PP-homopolymer to a poly(propylene-*co*-ethylene) random copolymer (PP-copolymer) known to exhibit better elastic properties, a noticeable improvement in the compressive fatigue behavior of the open-cell foam is seen. Figure 5b shows the stress−strain behavior of open-cell foams prepared from PP-copolymer/PTFE fibrillar blend and the inset shows the morphology of the obtained open-cell foams. Upon 60% compression, PP-copolymer/PTFE open-cell foam reaches a maximum stress of 45 kPa, which is lower than the maximum stress of the PP-homopolymer/PTFE open-cell foam (70 kPa), indicating that the PP-copolymer/PTFE open-cell foam is softer. Figure 5c compares the permanent strain undergone by the PP-homopolymer/PTFE open-cell foam sample with the permanent strain undergone by the PP-copolymer/PTFE open-cell foam sample, as a function of the compressive cycle number. The PP-copolymer/PTFE foam undergoes a smaller percentage permanent strain over the ten compressive cycles (about 10%) than the PP-homopolymer/PTFE foam (about 30%). This indicates that the PP-copolymer/PTFE foam demonstrates better recovery to its original shape after a compressive cycle than the PP-homopolymer/PTFE open-cell foam and has a superior reusability after mechanical "squeezing" required for extracting oil from the open-cell foam. The PP-copolymer/PTFE foam demonstrates similar uptake capacities, morphological characteristics and can be

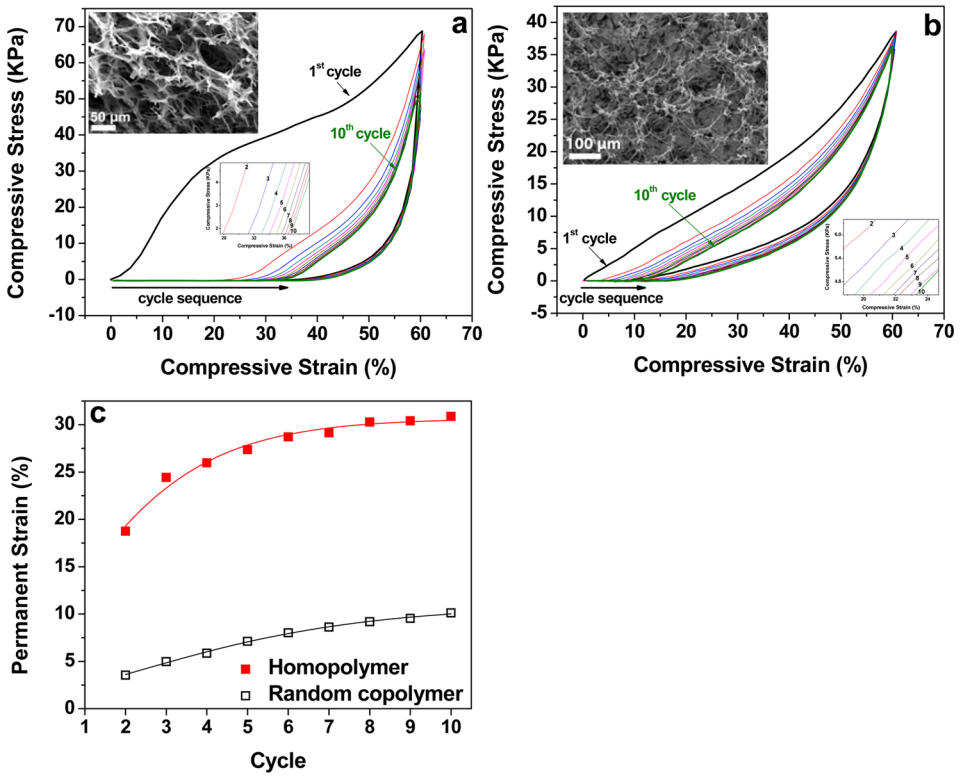

Figure 5. Mechanical behavior of PP-homopolymer/PTFE and PP-copolymer/PTFE open-cell foams: (a) Stress−strain curves of the open-cell foams made from PP-homopolymer/PTFE in the process of ten cyclic compressions. The SEM micrograph shows the morphology of the PP-homopolymer/PTFE open-cell foam. The compression cycle sequence is numbered in the inset. An arrow is also included to show the cycle sequence from 1st compression to the 10th compression; (b) stress−strain curves of the open-cell foams made from PP-copolymer/PTFE in the process of ten cyclic compressions. The SEM micrograph shows the morphology of the PP-copolymer/PTFE open-cell foam. The compression cycle sequence is numbered in the inset. An arrow is also included to show the cycle sequence from 1st compression to the 10th compression; and (c) permanent strain undergone by the PP-homopolymer/PTFE open-cell foam and PP-copolymer/PTFE open-cell foam as a function of cycle number. PP-homopolymer/PTFE open-cell foams undergo a permanent deformation of 30% while PP-copolymer/PTFE open-cell foams undergo a permanent deformation of 10% over the 10 compressive cycles.

prepared under similar processing conditions as the PP-homopolymer/PTFE open-cell foams (see SI Figure S3 and Tables S1 and S2).

3.6. Kinetics of Oil Uptake. The extruded open-cell foams have a thin, impervious "skin" layer which offers low oil permeability. The uptake of oil occurs predominantly from the open-cell core which becomes exposed when the filament is cut into cross sections. In order to increase the porosity of the unfoamed skin layer and enhance the rate of oil uptake, high intensity ultrasound has been previously successfully employed.[15−17,45−47] Such morphological changes occur due to a phenomenon known as *ultrasonic cavitation*[46] near solid surfaces in a liquid. Ultrasonic cavitation is the formation and violent collapse of small bubbles in the liquid as a result of pressure changes in the medium. The collapse of bubbles near solid surfaces can generate fast-moving liquid microjets directed toward the surface. The impact of the jets on the surface can create localized damage. We employ high intensity ultrasound to increase the porosity of the impervious "skin" layer of the extruded foam. Figure 6a shows the SEM micrographs of the PP-homopolymer/PTFE open-cell foam skin layer before ultrasound irradiation treatment and after the ultrasound irradiation treatment. Prior to treatment, the surface shows a relatively nonporous structure. However, post-treated samples exhibit pronounced surface porosities. Ultrasonic irradiation treatment has been reported to cause site-specific chain scission in polymers by cleaving weak peroxide,[48] azo[49] and coordination bonds.[50] Ultrasonic degradation of PP has been observed in solution[51] and in the melt state.[52] However, the effect of ultrasonic irradiation treatment on solid-state PP remains unclear. Measurements of the complex viscosity of the open-cell PP/PTFE foam before and after the ultrasonic irradiation treatment are conducted and reveal that ultrasonic irradiation does not affect the complex viscosity of PP/PTFE (see SI Figure S4) and chemical changes such as chain scission and degradation are not significant.

Figure 6b,c shows the uptake rate of gasoline and the uptake rate of diesel, respectively, for the open-cell foams before ultrasound treatment and after ultrasound treatment. The open-cell foam takes a shorter time to saturate with gasoline than to saturate with diesel, both before and after ultrasound irradiation treatment. The more rapid uptake of gasoline compared to diesel is due to the lower viscosity of gasoline which allows it to infiltrate into the open-cell foam structure more easily. After ultrasound irradiation treatment, the open-cell foams demonstrate more rapid oil uptake rates for both gasoline and diesel due to the increased permeability of oil through the opened "skin" layer. The uptake kinetics can be described by the second order equation:

$$\frac{1}{Q_e - Q_t} = \frac{1}{Q_e} + kt \quad (1)$$

dx.doi.org/10.1021/am506006v | ACS Appl. Mater. Interfaces 2014, 6, 21131−21140

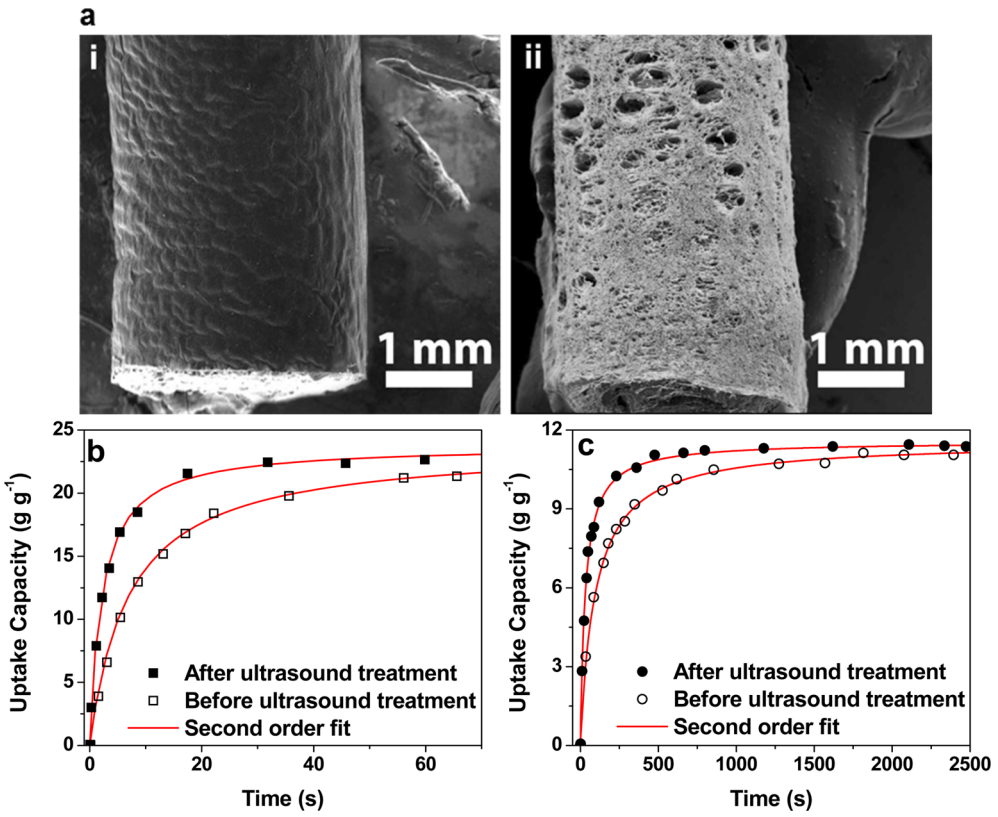

Figure 6. Enhancing kinetics of oil absorption of PP-homopolymer/PTFE open-cell foams: (a) SEM micrographs of the "skin" layer of the extruded open-cell foams, (i) before high intensity ultrasound treatment, (ii) after high intensity ultrasound treatment; (b) Gasoline uptake as a function of time for the open-cell foam before and after ultrasound treatment; (c) Diesel uptake as a function of time for the open-cell foam before and after ultrasound treatment.

where Q_e is the equilibrium uptake capacity corresponding to when the foam is completely saturated, Q_t is the uptake capacity at time t, and k is the uptake capacity rate constant. The curves of best-fit are included in Figure 6b,c and the corresponding fitting values of Q_e and k for the two petroleum products are presented in Table 3. The coefficients of determination R^2, for all curves are >0.99 indicating excellent agreement between the second order uptake kinetics model and the experimental data.

Table 3. Fitting Parameters for Uptake Kinetics of Gasoline and Diesel

petroleum product	foam treatment	Q_e (g g^{-1})	$k \times 10^3$ (g g^{-1} s^{-1})
gasoline	unsonicated	23.8	6
gasoline	sonicated	23.2	19
diesel	unsonicated	11.6	0.9
diesel	sonicated	11.9	2.7

4. CONCLUSIONS

Superior superhydrophobic and oleophilic open-cell foams of PP/PTFE (97/3 wt %) fibrillar blends, are prepared. The open-cell foams display significant improvements in oil uptake capacities compared to commercially available PP-based materials currently used for oil-spill cleanup applications, such as nonwoven PP fibers and melt-blown PP pads. These open-cell foams exhibit superhydrophobicity and oleophilicity which results in a high oil/water selectivity. The open-cell foams have a low density of about 0.07 g cm^{-3}, which makes the foams highly buoyant in water. The open-cell foams also have a high void fraction of 0.92 which makes available a large 3D space for oil storage. The open-cell foams offer robust stability at temperatures ranging from −196 to 120 °C. Subjecting the open-cell foams to these temperature extremes for prolonged periods does not influence the superhydrophobic and oleophilic properties of the foams. The kinetics of oil uptake can be enhanced by increasing the "skin" layer porosity of the extruded foams using high intensity ultrasound irradiation treatment. If the PP matrix in the PP/PTFE fibrillar blend is a PP-homopolymer, then the reusability of the foams is poor because PP-homopolymer/PTFE undergoes a large permanent deformation after mechanical "squeezing" to extract the oil (30% permanent deformation over ten compression cycles). This damages the open-cell morphology and consequently, the superhydrophobic and oleophilic properties. If the PP matrix in the PP/PTFE fibrillar blend is a PP random-copolymer, then the reusability of the foams is drastically improved because the resultant PP-copolymer/PTFE open-cell foams undergo a small permanent deformation after mechanical squeezing to extract the oil (10% permanent deformation over ten compressive cycles). The open-cell foams are prepared using conventional foam extrusion equipment and low-cost, commercially available raw materials. Consequently, the fabrication process is easy to scale-up. The open-cell foams are technologically promising for applications such as oil-spill cleanup, organic pollutant removal, and field water remediation.

■ ASSOCIATED CONTENT

Supporting Information

Photograph of the tandem foam extrusion system, SEM image showing the formation of crystalline heterogeneities during extrusion, complex viscosity of PP/PTFE open-cell foams before and after ultrasonic irradiation treatment to determine degradation of PP, comparison of oil uptake performance for PP-homopolymer/PTFE and PP-copolymer/PTFE open-cell foams, video of the extrusion of open-cell PP/PTFE foams, and video of the selective uptake of oil by the extruded open-cell foam. This material is available free of charge via the Internet at http://pubs.acs.org/.

■ AUTHOR INFORMATION

Corresponding Author

*E-mail: park@mie.utoronto.ca.

Notes

The authors declare no competing financial interest.

■ ACKNOWLEDGMENTS

The authors would like to thank the members of the Consortium of Cellular and Microcellular Plastics (CCMCP) for their financial support of this project. The authors would also like to thank Nobuhisa Takayama from Mitsubishi Rayon Co. Ltd. and Japan Polypropylene Corp. for material donation. A.R. thanks the NSERC (Canada) for providing the CGS-D2 scholarship.

■ REFERENCES

(1) Shen, K. Z.; Yang, W.; Huang, R.; Yang, M. B. Transcrystalline Morphology of an In Situ Microfibrillar Poly(ethylene terephthalate)/Poly(propylene) Blend Fabricated through a Slit Extrusion Hot Stretching-Quenching Process. *Macromol. Rapid Commun.* **2004**, *25*, 553−558.

(2) Zhang, X. D.; Neff, R. A.; Macosko, C. W. Foam Stability in Flexible Polyurethane Foam Systems. In *Polymeric Foams, Mechanisms and Materials*; Lee, S. T., Ramesh, N. S., Eds.; CRC Press: Boca Raton, FL, 2004; pp 139−172.

(3) Choi, H. M.; Cloud, R. M. Natural Sorbents in Oil Spill Cleanup. *Environ. Sci. Technol.* **1992**, *26*, 772−776.

(4) Radetić, M. M.; Jocić, D. M.; Jovančić, P. M.; Petrović, Z. L.; Thomas, H. F. Recycled Wool-Based Nonwoven Material as an Oil Sorbent. *Environ. Sci. Technol.* **2003**, *37*, 1008−1012.

(5) Annunciado, T. R.; Sydenstricker, T. H. D.; Amico, S. C. Experimental Investigation of Various Vegetable Fibers as Sorbent Materials for Oil Spills. *Mar. Pollut. Bull.* **2005**, *50*, 1940−1346.

(6) Duong, H. T. T.; Burford, R. P. Effect of Foam Density, Oil Viscosity, and Temperature on Oil Sorption Behavior of Polyurethane. *K. Appl. Polym. Sci.* **2006**, *99*, 360−367.

(7) Zhu, Q.; Pan, Q.; Liu, F. Facile Removal and Collection of Oils from Water Surfaces through Superhydrophobic and Superoleophilic Sponges. *J. Phys. Chem. C* **2011**, *115*, 17464−17470.

(8) Zhu, Q.; Chu, Y.; Wang, Z.; Chen, N.; Lin, L.; Liu, F.; Pan, Q. Robust Superhydrophobic Polyurethane Sponge as a Highly Reusable Oil-Absorption Material. *J. Mater. Chem. A* **2013**, *1*, 5386−5393.

(9) Camilli, L.; Pisani, C.; Gautron, E.; Scarselli, M.; Castrucci, P.; D'Orazio, F.; Passacantando, M.; Moscone, D.; Crescenzi, M. D. A Three-Dimensional Carbon Nanotube Network for Water Treatment. *Nanotechnology* **2014**, *25*, 1−7.

(10) Bi, H.; Xie, X.; Yin, K.; Zhou, Y.; Wan, S.; He, L.; Xu, F.; Banhart, F.; Sun, L.; Ruoff, R. S. Spongy Graphene as a Highly Efficient and Recyclable Sorbent for Oils and Organic Solvents. *Adv. Funct. Mater.* **2012**, *22*, 4421−4425.

(11) Lei, W.; Portehault, D.; Liu, D.; Qin, S.; Chen, Y. Porous Boron Nitride Nanosheets for Effective Water Cleaning. *Nat. Commun.* **2013**, *4*, 1−7.

(12) Yang, C.; Kaipa, U.; Mather, Q. Z.; Wang, X.; Nesterov, V.; Venero, A. F.; Omary, M. A. Fluorous Metal−Organic Frameworks with Superior Adsorption and Hydrophobic Properties toward Oil Spill Cleanup and Hydrocarbon Storage. *J. Am. Chem. Soc.* **2011**, *133*, 18094−18097.

(13) Hayase, G.; Kanamori, K.; Fukuchi, M.; Kaji, H.; Nakanishi, K. Facile Synthesis of Marshmallow-Like Macroporous Gels Usable Under Harsh Conditions for the Separation of Oil and Water. *Angew. Chem.* **2013**, *52*, 1986−1989.

(14) Park, C. B.; Suh, N. P. Filamentary Extrusion of Microcellular Polymers. *Polym. Eng. Sci.* **1996**, *36*, 34.

(15) Wang, X.; Li, W.; Kumar, V. A Method for Solvent-Free Fabrication of Porous Polymer using Solid-State Foaming and Ultrasound for Tissue Engineering Applications. *Biomaterials* **2006**, *27*, 1924−1929.

(16) Guo, G.; Ma, Q.; Zhao, B.; Zhang, D. Ultrasound-Assisted Permeability Improvement and Acoustic Characterization for Solid-State Fabricated PLA Foams. *Ultrason. Sonochem.* **2013**, *20*, 137−143.

(17) Watson, N. J.; Johal, R. K.; Glover, Z.; Reinwald, Y.; White, L. J.; Ghaemmaghami, A. M.; Morgan, S. P.; Rose, F. R. A. J.; Povey, M. J. W.; Parker, N. G. Post-Processing of Polymer Foam Tissue Scaffolds with High Power Ultrasound: A Route to Increased Pore Interconnectivity, Pore Size and Fluid Transport. *Mater. Sci. Eng., C* **2013**, *33*, 4825−4832.

(18) Ali, M. A.; Nobukawa, S.; Yamaguchi, M. Morphology Development of Polytetrafluoroethylene in a Polypropylene Melt (IUPAC Technical Report). *Pure Appl. Chem.* **2011**, *83*, 1819−1830.

(19) Rizvi, A.; Tabatabaei, A.; Barzegari, R.; Mahmood, H.; Park, C. B. In-Situ Fibrillation of CO_2-Philc Polymers: Sustainable Route to Polymeric Foams in a Continuous Process. *Polymer* **2013**, *54*, 4645−4652.

(20) Park, C. B.; Baldwin, D. F.; Suh, N. P. Effect of the Pressure Drop Rate on Cell Nucleation in Continuous Processing of Microcellular Polymers. *Polym. Eng. Sci.* **1995**, *35*, 432−440.

(21) Xu, X.; Park, C. B.; Xu, D.; Pop-Iliev, R. Effect of Die Geometry on Cell Nucleation of PS Foams Blown with CO_2. *Polym. Eng. Sci.* **2003**, *43* (7), 1378−1390.

(22) Li, Y. G.; Park, C. B.; Li, H. B.; Wang, J. Measurement of the PVT Property of PP/CO_2 Solution. *Fluid Phase Equilib.* **2008**, *270*, 15−22.

(23) Ali, M.; Okamoto, K.; Yamaguchi, M.; Kasai, T.; Koshirai, A. Rheological Properties for Polypropylene Modified by Polytetrafluoroethylene. *J. Polym. Sci., Part B: Polym. Phys.* **2009**, *47*, 2008−2014.

(24) Rizvi, A.; Park, C. B.; Yamaguchi, M. Resin Composition Foam and Method for Producing Same. WO2013137301, March 13, 2013.

(25) Binsbergen, F. L. Orientation-Induced Nucleation in Polymer Crystallization. *Nature* **1966**, *211*, 516−517.

(26) Lee, P. C.; Wang, J.; Park, C. B. Extruded Open-Cell Foams using Two Semicrystalline Polymers with Different Crystallization Temperatures. *Ind. Eng. Chem. Res.* **2006**, *45*, 175−181.

(27) Lee, P. C.; Wang, J.; Park, C. B. Extrusion of Microcellular Open-Cell LDPE-Based Sheet Foams. *J. Appl. Polym. Sci.* **2006**, *102*, 3376−3384.

(28) Harikrishnan, G.; Patro, T. U.; Khakhar, D. V. Polyurethane Foam−Clay Nanocomposites: Nanoclays as Cell Openers. *Ind. Eng. Chem. Res.* **2006**, *45*, 7126−7134.

(29) Lee, P. C.; Naguib, H. E.; Park, C. B.; Wang, J. Increase of Open-Cell Content by Plasticizing Soft Regions with Secondary Blowing Agent. *Polym. Eng. Sci.* **2005**, *45*, 1445−1451.

(30) Park, C. B.; Padareva, V.; Lee, P. C.; Naguib, H. E. Extruded Open-Celled LDPE-Based Foams using Non-Homogeneous Melt Structure. *J. Polym. Eng.* **2005**, *25*, 239−260.

(31) Sing, K. S. W.; Everett, D. H.; Haul, R. A. W.; Moscou, L.; Pierotti, R. A.; Rouquerol, J.; Siemieniewska, T. Reporting Physisorption Data for Gas/Solid Systems with Special Reference to

the Determination of Surface Area and Porosity. *Pure Appl. Chem.* **1985**, *57*, 603−619.
(32) Wang, S.; Jiang, L. Definition of Superhydrophobic States. *Adv. Mater.* **2007**, *19*, 3423−3424.
(33) Cassie, A. B. D.; Baxter, S. Wettability of Porous Surfaces. *Trans. Faraday Soc.* **1944**, *40*, 546−551.
(34) Li, X. M.; Reinhoudt, D.; Crego-Calama, M. What Do We Need for a Superhydrophobic Surface? A Review on the Recent Progress in the Preparation of Superhydrophobic Surfaces. *Chem. Soc. Rev.* **2007**, *36*, 1350−1368.
(35) Adebajo, M. O.; Frost, R. L.; Kloprogge, J. T.; Carmody, O.; Kokot, S. Porous Materials for Oil Spill Cleanup: A Review of Synthesis and Absorbing Properties. *J. Porous Mater.* **2003**, *10*, 159−170.
(36) Wei, Q. F.; Mather, R. R.; Fotheringham, A. F.; Yang, R. D. Evaluation of Nonwoven Polypropylene Oil Sorbents in Marine Oil-Spill Recovery. *Mar. Pollut. Bull.* **2003**, *46*, 780−783.
(37) Teas, C.; Kalligeros, S.; Zanikos, F.; Stournas, S.; Lois, E.; Anastopoulos, G. Investigation of the Effectiveness of Absorbent Materials in Oil Spills Clean Up. *Desalination* **2001**, *140*, 259−264.
(38) Bayat, A.; Aghamiri, S. F.; Moheb, A.; Vakili-Nezhaad, G. R. Oil Spill Cleanup from Sea Water by Sorbent Materials. *Chem. Eng. Technol.* **2005**, *28*, 1525−1528.
(39) Chung, T. C.; Yuan, X. P. Methods and Materials for Hydrocarbon Recovery. WO 2012024614 A2, February 23, 2012.
(40) Zhao, J.; Xiao, C.; Xu, N. Evaluation of Polypropylene and Poly(butylmethacrylate-*co*-hydroxyethylmethacrylate) Nonwoven Material as Oil Absorbent. *Environ. Sci. Pollut. Res.* **2013**, *20*, 4137−4145.
(41) Pan, Y.; Shi, K.; Peng, C.; Wang, W.; Liu, Z. J. X. Evaluation of Hydrophobic Polyvinyl-Alcohol Formaldehyde Sponges as Absorbents for Oil Spill. *ACS Appl. Mater. Interfaces* **2014**, *6*, 8651−8659.
(42) Wu, Z. Y.; Li, C.; Liang, H. W.; Zhang, Y. N.; Wang, X.; Chen, J. F.; Yu, S. H. Carbon Nanofiber Aerogels for Emergent Cleanup of Oil Spillage and Chemical Leakage Under Harsh Conditions. *Sci. Rep.* **2014**, *4*, 1−6.
(43) Dasari, A.; Rohrmann, J.; Misra, R. D. K. Microstructural Aspects of Surface Deformation Processes and Fracture of Tensile Strained High Isotactic Polypropylene. *Mater. Sci. Eng. A-Struct.* **2003**, *358*, 372−383.
(44) Maier, C.; Calafut, T. *Polypropylene—The Definitive User's Guide and Databook*, 1st ed.; William Andrew Publishing/Plastics Design Library: Norwich, NY, 1998.
(45) Gandhi, A.; Asija, N.; Gaur, K. K.; Rizvi, S. J. A.; Tiwari, V.; Bhatnagar, N. Ultrasound Assisted Cyclic Solid-State Foaming for Fabricating Ultra-low Density Porous Acrylonitrile−Butadiene−Styrene Foams. *Mater. Lett.* **2013**, *94*, 76−78.
(46) Benjamin, T. B.; Ellis, A. T. The Collapse of Cavitation Bubbles and the Pressure Thereby Produced Against Solid Boundaries. *Philos. Trans. R. Soc. London A* **1966**, *260*, 221−245.
(47) Wang, X.; Li, W.; Kumar, V. Creating Open-Celled Solid-State Foams using Ultrasound. *J. Cell. Plast.* **2009**, *45*, 353−369.
(48) Encina, M. V.; Lissi, E.; Sarasua, M.; Gargallo, L.; Radic, D. Ultrasonic Degradation of Polyvinylpyrrolidone—Effect of Peroxide Linkages. *J. Polym. Sci., Polym. Lett. Ed.* **1980**, *18*, 757−760.
(49) Berkowski, K. L.; Potisek, S. L.; Hickenboth, C. R.; Moore, J. S. Ultrasound-Induced Site-Specific Cleavage of Azo-Functionalized Poly(ethylene glycol). *Macromolecules* **2005**, *38*, 8975−8978.
(50) Paulusse, J. M. J.; Sijbesma, R. P. Reversible Mechanochemistry of a Pd-II Coordination Polymer. *Angew. Chem., Int. Ed.* **2004**, *49*, 4460−4462.
(51) Desai, V.; Shenoy, M. A.; Gogate, P. R. Degradation of Polypropylene using Ultrasound-Induced Acoustic Cavitation. *Chem. Eng. J.* **2008**, *140*, 483−487.
(52) Kim, H.; Lee, J. W. Effect of Ultrasonic Wave on the Degradation of Polypropylene Melt and Morphology of its Blend with Polystyrene. *Polymer* **2002**, *43*, 2585−2589.